Oxidation of Metals, Vol. 59, Nos. 5/6, June 2003 (© 2003)

Sulfur Segregation to Al_2O_3–FeAl Interfaces Studied by Field Emission-Auger Electron Spectroscopy

P. Y. Hou* and J. Moskito†

Received June 11, 2002

Using a 30-nm field-emission Auger spectroscopy probe, the segregation of sulfur to a growing oxide–metal interface was studied. The interfaces were formed by the oxidation of a Fe–40at.% Al alloy at 1000°C for various times. Both the oxide and the alloy sides of the interface were examined after spalling the surface Al_2O_3 layer in ultra-high vacuum. Results were compared with similar studies performed using conventional AES and related to scale development and the interface microstructure. Sulfur started to segregate to the interface only after a complete layer of α-Al_2O_3 developed there, its concentration then increased slowly with further oxidation until reaching a level close to half a monolayer. Higher amounts were observed on interfacial-void surfaces, where Al and S cosegregated. The study showed that sulfur segregation to oxide–alloy interfaces depended on the type of interface, indicating possible relationships between segregation energies and interface microstructure.

KEY WORDS: auger electron microscopy; iron alloys; surfaces and interfaces; oxidation; segregation.

INTRODUCTION

All commercial metals and alloys contain small amounts of nonmetallic impurities, such as C, N, and S, which readily segregate to surfaces when the alloys are heated in vacuum. The type and the amount segregated are functions of temperature and time, which depend on the impurity concentration, the segregation free energy, and the diffusion rate of the segregant.[1]

*Materials Sciences Division, Lawrence Berkeley National Laboratory, Berkeley, California 94720
†Charles Evans and Associates, Sunnyvale, California 94086.

0030-770X/03/0600-0000/0

Similar segregation occurs on alloy grain boundaries, usually to a lesser degree, and the coverage often depends on grain-boundary structures.[2–4] Under the operating temperatures, 900–1150°C, of heat-resisting alloys that form Al_2O_3 scales, sulfur is expected to segregate to the alloy surface.[5] However, in an oxidizing environment, where a surface-oxide layer always exists, it is uncertain if similar segregation would occur at the oxide–metal interface.

As it is well known that S segregation at metal grain boundaries causes boundary embrittlement,[6–8] it was proposed over a decade ago that sulfur also segregates to growing oxide–metal interfaces to weaken the interfacial bonds and reduce scale adhesion.[9] Subsequent studies on H_2-annealed alloys[10–14] or those containing very low sulfur concentrations[15,16] have demonstrated that removing sulfur in the alloy, indeed, improves oxide-scale adhesion. However, the phenomenon of impurity segregation to a growing oxide–alloy interface in relation to interface structure and strength has received little attention. Questions have been raised concerning whether a large sulfur ion is energetically favorable to segregate to a well-bonded oxide–metal interface.[17] Other important questions pertinent to understanding factors affecting scale adhesion include the rate, content, type, and structure of any impurity present at the interface. Furthermore, in light of the dynamic nature of the growing scale, it is also essential to understand how the segregation process is related to oxide growth.

The build up of S with oxidation time has been studied using conventional Auger spectroscopy (AES) on Al_2O_3/FeCrAl, Fe_3Al, FeAl[18–21] and on Cr_2O_3/Cr[18] interfaces after the surface scales were removed by scratching in ultra-high vacuum (UHV). Results on FeAl showed that sulfur did not segregate to the scale–alloy interface until a complete layer of α-Al_2O_3 formed at the interface. Its concentration then built up slowly with oxidation time.[21] This finding seems to indicate that sulfur not only segregates to growing oxide–metal interfaces, but the process is strongly related to scale development. However, as one observes the microstructure of the alloy surface after scale removal, as those shown later in Figs. 3 and 5, it appears that very small voids may exist between the facets imprinted by α-Al_2O_3 grains. A 0.5-1-μm Auger probe can easily include these voids, whose surface is expected to have saturated amounts of sulfur. Hence, S would be detected and more of these voids may exist with longer oxidation times to produce the apparent increase in S concentration at the interface. Therefore, in order to truly determine whether sulfur segregates to oxide–metal interfaces, individual facets at the alloy surface made by imprints of the Al_2O_3 grain above them should be analyzed. The purpose of this paper is to report results of this kind using field-emission (FE) AES with a probe

size of 30 nm. Results from conventional AES are presented for comparison, with a brief summary of scale development.

EXPERIMENTAL METHODS

The Fe–Al alloy, from Oak Ridge National Laboratory, was prepared by arc melting and casting, followed by hot rolling to a ~1 mm-thick sheet. The alloy contains 40 at.% aluminum and 20 ppm by weight of sulfur impurity. It was annealed in He at 1100°C for 50 hr before cutting into $15 \times 10 \times 1$ mm coupons. Specimens were polished to a 1-μm finish with diamond paste and cleaned ultrasonically in acetone prior to oxidation, which was carried out in a horizontal furnace in flowing, dry oxygen at 1000°C. Each specimen was placed in an alumina boat with a thermocouple attached at its back, equilibrated with the oxygen flow, then inserted into the hot zone to be oxidized for times ranging from 1 min to 24 hr. At the end of the desired oxidation time, the boat and specimen were quickly pulled out of the furnace and cooled in ambient air. Cooling to 500°C took about 1.3 min; cooling to 300°C took an additional 2 min. One specimen was furnace-cooled in argon gas to establish different cooling rates. The furnace cooling had a linear rate of 3.9°C/min from 1000 to 300°C.

The surface-oxide scale that formed after oxidation was characterized using X-ray diffraction (XRD), Auger depth profiling, and scanning-electron microscopy (SEM). Chemical analyses of the alloy and oxide sides of the interface were carried out using conventional and field-emission Auger electron spectroscopy (AES).

A PHI 660 conventional AES with a special scratch device was used. The device contained a Vickers micro-indenter mounted on a linear translator, and was placed in the UHV chamber to scratch the specimen surface under typically 10^{-10} Torr vacuum.[22] To begin a scratch, the indenter was first placed and secured above the specimen. An oxidized face was pushed into the indenter tip using the Z-control of the specimen stage to make an indent. Subsequent movement of the specimen holder along the X or the Y direction could then make a several millimeter long scratch on the surface. Such scratches, when applied with sufficient load, caused delamination and spallation of the oxide scale at numerous spots adjacent to the scratch mark, exposing the scale–alloy interface. An example is seen in Fig. 1a. A 0.5- to 1-μm diameter electron beam was then placed on the exposed metal surface to study its composition. Usually 10–15 areas were surveyed. With the attached scanning-electron microscope, the morphology of the surveyed area, such as interfacial voids, alloy grains, and grain boundaries, could be distinguished. The composition at the oxide side of the interface was determined by analyzing spalled-oxide pieces that turned over after spallation.

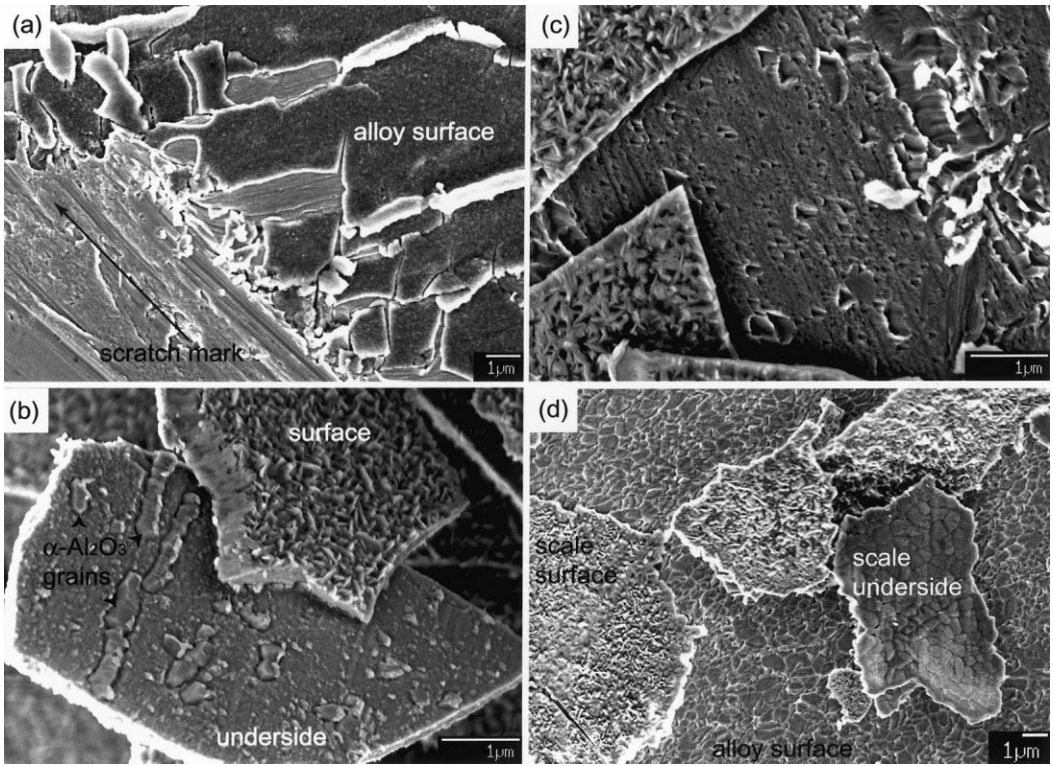

Fig. 1. SEM micrographs showing scale development with oxidation time. (a) After 3 min with scratch-induced spallation; (b), (c) after 10 min, with (b) showing top and bottom surfaces of the scale and (c) alloy surface beneath the scale; (d) scale and interface after 1 hr.

A similar scratch device was not available in the FE–AES PHI model 670 scanning Auger microprobe system, so the parking stage arm inside the chamber was used to remove already spallation prone scales to expose the alloy surface. These are scales formed at 1000°C for more than 1 hr. With a typical probe size of 30 nm, individual facets on the alloy surface made by oxide grain imprints could be analyzed, providing much greater spatial resolution. An unoxidized FeAl specimen was analyzed as standards for the Fe and Al concentrations in the alloy. Since sputtering preferentially removed Al, a light scratch by the parking-stage arm was used to remove any surface oxide present at room temperature to obtain consistent and more accurate data on the starting material.

RESULTS

Morphologies of the oxide scale and the scale–alloy interface after different oxidation times are shown in Fig. 1. In Fig. 1a, the specimen was oxidized for 3 min, forming a scale less than 0.2 μm thick that consisted of a single Al_2O_3 layer. The alumina that formed at this early stage was cubic, identified by XRD to be θ and γ-Al_2O_3, rather than the more stable α form. The thin oxide cracked and delaminated under the force of the scratch made in vacuum. Spallation of the oxide pieces exposed the alloy surface, which was smooth and featureless, on which AES analysis found only Al and Fe, as seen in Fig. 2a.

After 10 min (Fig. 1b), whiskers of about 0.2–0.3 μm, which are typical of the cubic transition alumina,[23] can be seen on the outer surface and crystalline grains. These whiskers start to appear at random locations on the scale underside. According to past TEM experiences,[24,25] these grains should be α-Al_2O_3 that nucleated at the scale–alloy interface. Imprints of these grains are seen on the surface of the alloy (Fig. 1c), which was again free from any impurity, whether on the smooth part beneath the cubic alumina or the faceted areas that were in contact with the α-Al_2O_3.

After 1-hr oxidation (Fig. 1d), XRD analysis showed that the scale consisted mainly of α-Al_2O_3. Whiskers on the outer oxide surface became less apparent, the scale underside was covered with α-Al_2O_3 grains, and the alloy surface showed imprints that corresponded in shape and size to these grains. This type of morphology persisted with further oxidation time with little oxide grain growth at the scale–alloy interface.[26] Small amounts of sulfur were detected everywhere on the alloy surface after 1-hr oxidation; an Auger spectrum is shown in Fig. 2b. On the underside of the scale, i.e., the oxide side of the interface, only Al and O were detected (Fig. 2d); this was true regardless of the oxidation time. Splitting of the low-energy Al peak seen in Fig. 2(d) was due to slight surface charging.

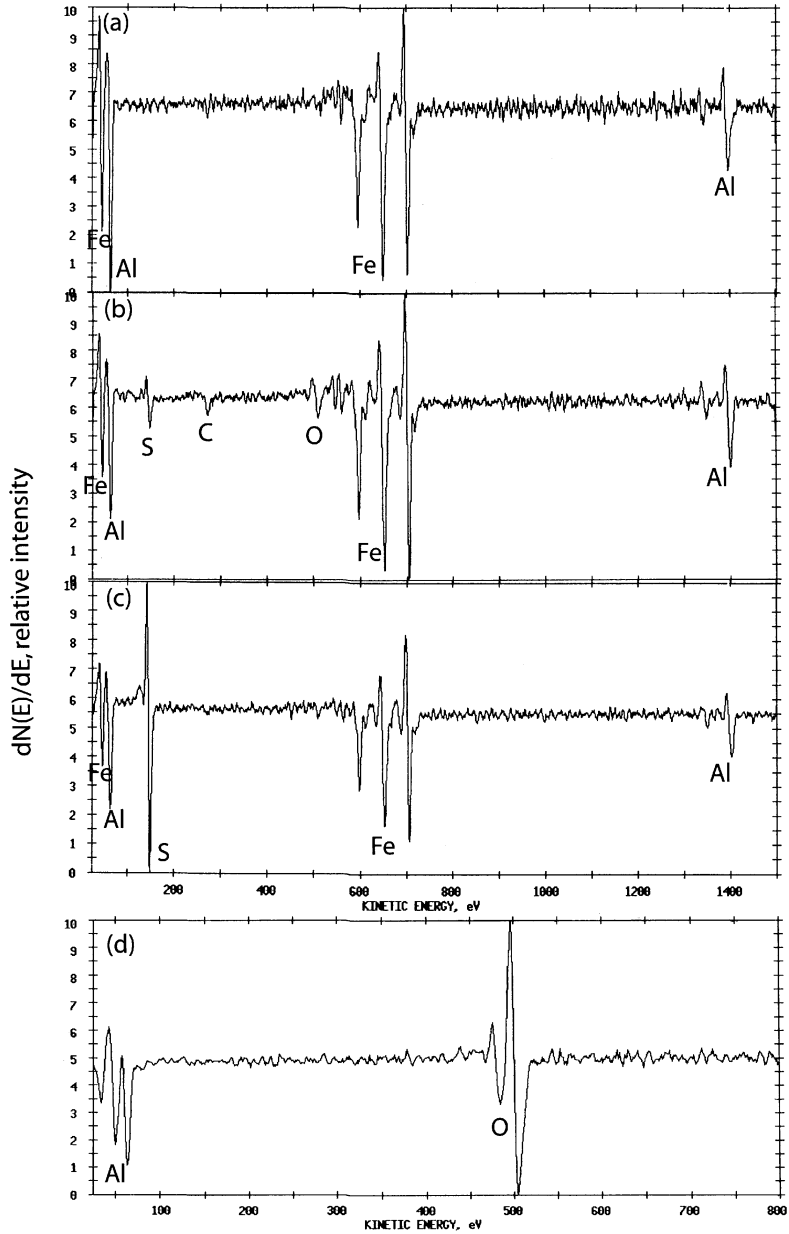

Fig. 2. Spectra of the Al_2O_3–FeAl interface examined using conventional AES after scale removal in vacuum. Alloy side after (a) 3 min and (b) 1-hr oxidation; (c) surface of large micron-sized voids; (d) oxide side after all oxidation times.

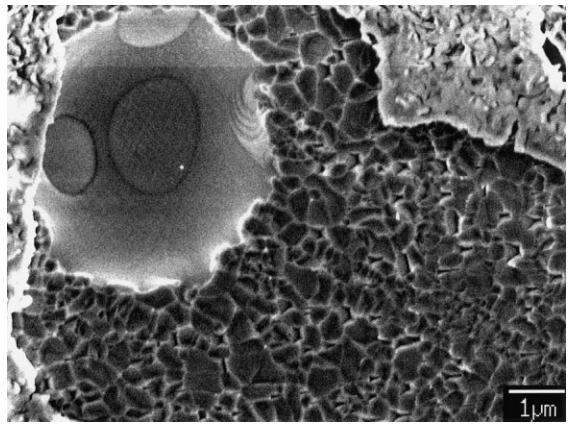

Fig. 3. SEM micrograph of a large micron-sized void with neighboring oxide-imprinted region at the scale–alloy interface after 1-hr oxidation.

Voids several microns in diameter and more than an order of magnitude larger than the oxide grains (an example is shown in Fig. 3), were always found on the alloy surface beneath the external scale. Their surfaces had a much higher concentration of sulfur (Fig. 2c) than on the neighboring oxide imprinted areas. The average sulfur content at the alloy surface, determined from conventional AES and calculated from Auger peak heights and tabulated sensitivity factors,[27] as a function of oxidation time is plotted as circles in Fig. 4. Initially, the interface was free from any impurity, although large interfacial void surfaces were covered with sulfur. After 1-hr oxidation, S began to appear at the interface. Its concentration increased with oxidation time and gradually reached saturation at about 10 at.% after 24 hr. The level of S on the large micron-sized void surfaces, on the other hand, was unchanged with time, reaching a constant level of more than 20 at.% after only 3 min of oxidation.

Summary of FE–AES results is also presented in Fig. 4. High levels of sulfur were again detected on the surfaces of large micron-sized interfacial voids. The interface area that consisted of many facets, as seen in Fig. 5, turned out to be a mixture of small voids and oxide imprints. Arrows on Fig. 5 mark the locations of voids. Their sizes are similar to that of the oxide imprints, but the voids had considerably higher levels of sulfur on their surfaces. The average amount of sulfur on grain facets increased slowly with a trend similar to that found by conventional AES, but at a lower level because there was no longer any contribution from the higher sulfur level on neighboring small voids. On the small voids that distributed among the

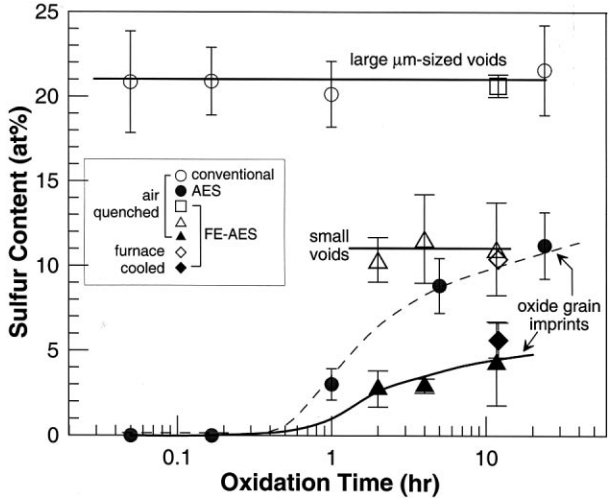

Fig. 4. Conventional and FE–AES results of S build up as a function of oxidation time on different features on alloy surfaces beneath an Al_2O_3 scale that was removed in UHV.

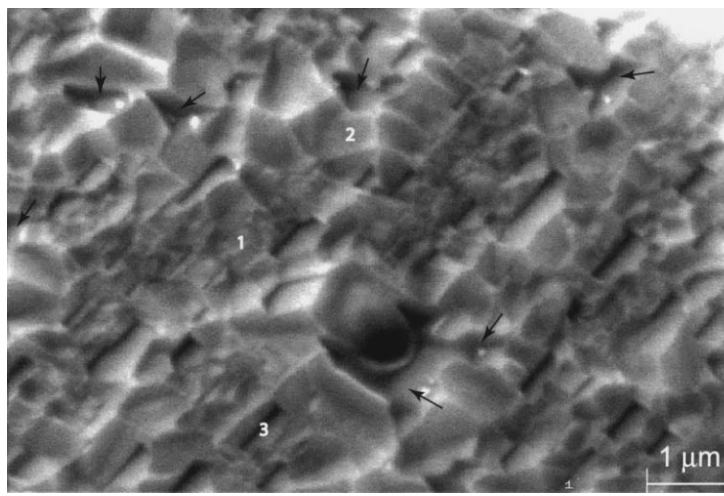

Fig. 5. SEM micrograph of an alloy surface after 2-hr oxidation examined using FE–AES. Arrows point to small interfacial voids. Numbers show types of oxide-imprinted areas that contained slightly different levels of S, as given in Table I.

imprints, the average sulfur level appeared to stay fairly constant with oxidation time, but, in fact, while evaluating all the experimental data, the amount of S on void surfaces actually increased with void size until it reached a very high level of about 20 at.% on the large micron-sized voids. The relationship between void size and the amount of S on its surface is shown in Fig. 6.

Within experimental errors, the slower cooling rate did not seem to alter the amount of sulfur present at the interface (Fig. 4). The same independence of cooling rate has also been shown on a Fe–Cr–Al alloy,[20] where the amount of interfacial sulfur remained unchanged with cooling rates that varied by a factor of 1000 through slow furnace cooling or water quenching.

Different shapes and orientations of interface facets that were imprinted by the oxide grain tend to have slightly different levels of sulfur. This result is summarized in Table I with three types of grains, whose examples are labeled by numbers in Fig. 5. It is seen that slight variations existed on different types of interfacial morphology and the S content increased with time on each type. Two alloy grains were analyzed on one sample, showing rather different S levels at the interface, indicating a possible substrate grain-orientation dependence.

The S that was present at the interface has been shown by depth profiling and X-ray photoelectron spectroscopy to be concentrated at the alloy surface.[28] The same is consistently shown with the current FE-AES data. In Fig. 7a the change in Fe surface concentration is plotted as a function of

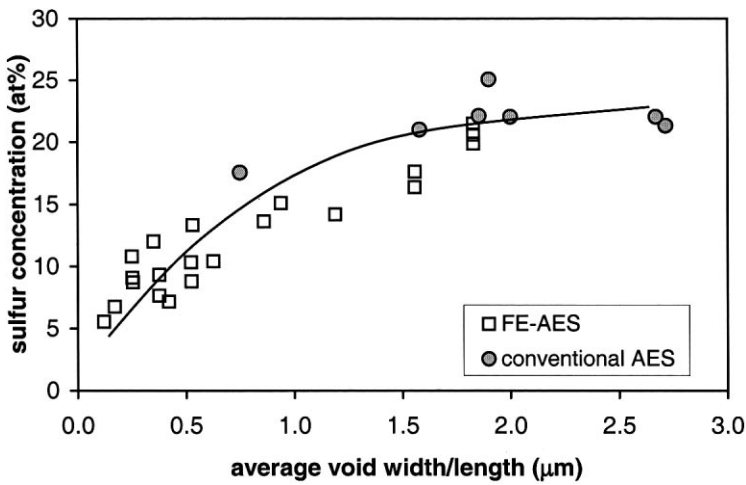

Fig. 6. Relationship between interfacial void size and the amount of S on void surfaces. Data are taken from different oxidation times.

Table I. Variation of Interface Sulfur Content with Microstructure and Oxidation Time

Description of interface	structure[a]	Oxidation condition				
				11.7 hr		
		2 hr	4 hr	Grain 1	Grain 2	12 hr[b]
Oxide	Fine (1)	1.53 ± 0.11				
grain	Flat (2)	2.40 ± 0.30	2.93 ± 0.42	1.36 ± 0.55	6.42 ± 0.59	
imprints	Slit (3)	4.31 ± 0.55		3.57 ± 0.32		5.63 ± 1.03

[a] Numbers as indicated on Fig. 5.
[b] Furnace cooled.

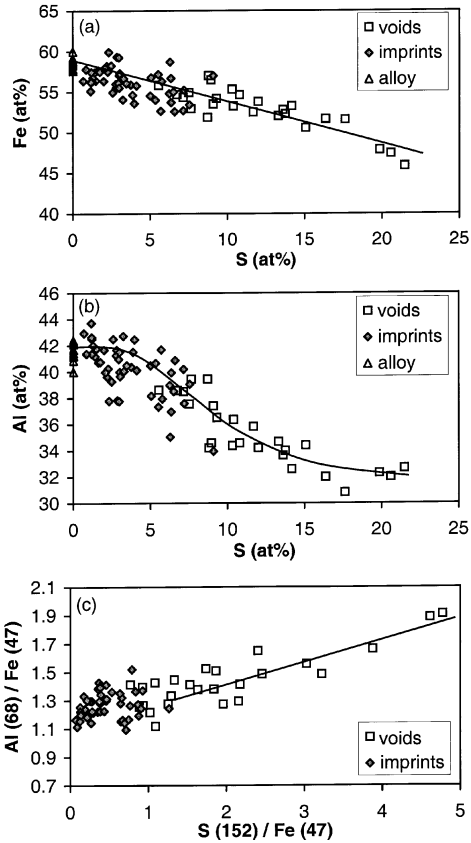

Fig. 7. Relationships of surface S, Fe, and Al concentrations, showing (a) a linear decrease of Fe with increasing S coverage, (b) the change of Al content as a function of S coverage, and (c) the cosegregation of Al and S on void surfaces.

Table II. Summary of Sulfur Coverage on Different Interfacial Structures

Interface structure	Fe(47) peak height	Average ratio Al(68)/Fe(47)	Average ratio S(152)/Fe(47)	Average S (at.%)	Approximate monolayer
Starting alloy	7.42 ± 0.17	1.17 ± 0.02	0	0	0
Oxide grain imprints	5.54 ± 0.52	1.23 ± 0.09	0.42 ± 0.25	3.46 ± 1.94	0.45 ± 0.15
Imprint sized voids	4.77 ± 0.69	1.36 ± 0.12	1.49 ± 0.51	9.95 ± 2.63	0.68 ± 0.23
Micron-sized voids	2.70 ± 0.52	1.70 ± 0.17	3.90 ± 0.71	19.17 ± 1.90	1.56 ± 0.31

sulfur content. A linear relationship is observed, indicating a constant attenuation of the Fe signal due to the build up of sulfur on the alloy surface. Similar results are also shown in Table II, where as the S content increased, the Fe peak heights decreased correspondingly. The surface aluminum content, however, did not change with small amounts of S segregation, as seen in Fig. 7b, but decreased quickly after about 5 at.% S at the alloy surface, and then leveled off after more than 11 at.% of S. Figure 7c shows peak-height ratios of Al/Fe and S/Fe for each surface analyzed. A linear relationship exists after an S/Fe ratio of ~1.5, which according to Table II is equivalent to ~10 at.% S, or ~1 monolayer. This linear relation indicates Al and S cosegregation, which did not seem to occur under low-sulfur coverage on oxide grain-imprinted areas. The Al content on the oxide–alloy interface was similar to that on the starting alloy, as seen from the Al/Fe ratio in Table II, but increased on void surfaces, suggesting that Al segregation occurs there.

Knowing that S is present at the surface of the alloy, a layer model of n layers with interlayer spacing d can be used to estimate its coverage.[29] The intensity of any Auger peak signal emitted by the element A in an alloy is given by

$$I_A = C\,(\sigma_A^{E_p}) R_A \sum_{n=0}^{\infty} N_A^{nd} \exp(-nd/\lambda_A \cos\theta) \tag{1}$$

where C is an instrument constant, $\sigma_A^{E_p}$ the ionization cross section of A at an operating electron energy E_p, R_A a backscatter term that depends on the matrix and the core electron energy, N_A^{nd} the number density of A atoms at depth nd, λ_A the elastic mean-free path, and θ the angle of emission from the surface normal.

The product $\lambda_A \cos\theta$ denotes the characteristic depth from which Auger electrons can be emitted. Thus, when sulfur and/or Al is adsorbed on the surface of Fe, I_{Fe} will be attenuated in proportion to $\exp(-nd/\lambda_A \cos\theta)$. Comparing the low-energy Fe signal intensity at 57 eV on each type of interface structure with that of the starting alloy, an approximate surface coverage could be determined and is given in the last

column of Table II. The level of coverage on oxide-grain imprints, or intact interfacial areas, was about 0.5 monolayer, and all of this should be attributed to S, since Al did not segregate to these surfaces. On the surface of small voids with similar size as the oxide imprints and large voids that were a few microns in diameter, the coverage was close to 1 and 1.5 monolayers, respectively. These values included some degree of Al cosegregation with sulfur, but the major contributor is still S. Exact quantification of the surface coverage requires data on S and Al surface adsorptions on the binary FeAl alloy, which are not available.

DISCUSSION

After pieces of α-Al_2O_3 scale grown above the FeAl alloy were mechanically removed in UHV, small probe FE-AES detected sulfur on every alloy facet that was examined, and the level was insensitive to the cooling rate. This result indicates that impurity segregation must have taken place at the oxide–alloy interface during scale growth. It is possible that parts of the scale delaminated due to stresses in the oxide film, causing S segregation to an alloy surface that was no longer in contact with the oxide.[30] This argument essentially states that the detected sulfur was a result of segregation to free alloy surfaces beneath a piece of detached scale. However, if that were the case, the amount of S found on the faceted grain imprints would not have been so uniform everywhere under every piece of scale that was mechanically removed. Usually, these pieces were more than 10 μm^2 in size, exposing a fairly substantial area. If this size of scale above the alloy were entirely delaminated, spallation of the piece would definitely occur during cooling due to the high thermal-mismatch stress between the Al_2O_3 scale and the underlying substrate.[14,31] The fact that scale pieces had to be scratched away indicates that some areas must still be in contact with the alloy prior to its removal in the AES vacuum chamber, and all areas were detected by FE–AES to contain sulfur.

Another possible source of sulfur at the interface is from interface sweeping. There, the oxide–metal interface moves inward with oxidation time as the alloy is consumed by oxidation and S in the alloy becomes incorporated onto the interface. Assuming that the oxidation process involved only inward-scale growth and the sulfur that was swept by the interface stayed and moved with it, the total amount of sulfur accumulated at the interface due to the oxidation process, J_S, can be determined from the sulfur content in the alloy, N_S, and the rate of scale thickening, or metal consumption, dh/dt:

$$J_s = c^o N_S \, dh/dt = c^o N_S [d(\Delta m/A)/dt]/c^o \nu M_O \tag{2}$$

where c^o is the alloy density in mole/cm^3, Δm/A the specimen weight gain per unit area from oxidation, ν the ratio between O and Al in Al_2O_3, and M_o the weight of oxygen. Taking the density of Fe–40 at.% Al[32] at 5.6 g/cm^3 with an approximate surface density of 1.8×10^{15} atoms/cm^2, and assuming one monolayer of sulfur coverage corresponds to about 11 at.% (Table II), J_S thus calculated is 0.8 at.% after 40 hr of oxidation. This level is much too low to account for the amount of S observed at oxide grain-imprinted areas. Results obtained from this work, therefore, indicated that sulfur could indeed segregate to growing oxide–alloy interfaces. This conclusion agrees with limited TEM observations that have detected S at intact oxide–metal interfaces without the presence of any pores. These include Cr_2O_3 grown on Cr[33], Al_2O_3 on NiAl,[34] and Al_2O_3 on Fe_3Al.[25] The last study was performed on a deposited amorphous Al_2O_3 film that transformed to θ or γ and then to α. Sulfur was detected at the α and the transition-alumina–alloy interfaces that were obviously void-free.

Combining FE and conventional AES results, the build up of sulfur at the Al_2O_3–FeAl interface was found to be much slower than that expected from segregation to free surfaces, as on interfacial voids. Micron-sized voids existed at the interface even for oxidation times as short as 3 min. Although how these voids nucleated at the early stage and grew to such a large size is not entirely understood, their surfaces clearly were covered with high levels of sulfur. The fact that this concentration could be achieved by as quickly as 3 min with oxidation time suggests that sulfur diffusion in the alloy was not rate limiting in this segregation process. During the first 10 min of oxidization, although all void surfaces were saturated with sulfur, none could be detected at oxide-imprinted areas, while the detection limit for S, calculated from signal-to-noise ratio, Auger sensitivity factors, and escape depths for Fe and S, was as good as 0.014 monolayer. Sulfur began to appear at these interfaces only with longer oxidation times; its concentration increased and slowly leveled off at times greater than 10 hr to about 5 at.%, which is equivalent to about 0.5 monolayer surface coverage.

The observed slow buildup at interfaces was not related to S diffusion rates in the alloy. Since oxidation is a dynamic process where new oxides form at the scale–alloy interface, and the interface progresses with time and with the scale-growth process, it is likely that the sulfur observed here is related to interface structures that change continuously with oxidation. Some indications of this can be seen from Fig. 5 and Table I, where alloy facets of similar shapes tend to have similar amounts of S. Thermodynamic-driving forces should dictate interfacial S segregation, like segregation to free surfaces. One possibility is that as the interface microstructure changes, segregation energy also changes, making it more favorable for S to segregate. Microscopically, this can be understood as an increase in the available

or preferential sites for segregation, as proposed by Hou *et al.*,[25] The process would be similar to that observed at alloy grain boundaries, where the extent of solute segregation often depends on the boundary structure,[2,3] with the tilt angle being the most significant factor.[4]

The details of how interface microstructure changes with oxidation have received little attention. The only system that had been characterized by high-resolution TEM was that of Al_2O_3 grown on NiAl.[24,35] Initially, transition alumina grew as a complete surface layer that formed a coherent interface with the alloy. With time, α-Al_2O_3 grains nucleated at the scale–alloy interface and established a complete layer. The α grains were randomly oriented with respect to the alloy, forming an incoherent interface.[35] If the extent of segregation were a strong function of interface coherency, it would be consistent with these TEM observations that S was not detected initially at transition alumina–alloy interfaces but only started to appear after α-Al_2O_3 formed. It should be noted that the interface between the alloy and the first-formed, isolated α-Al_2O_3 grains was clean. Only when a complete layer of α-Al_2O_3 grains formed at the interface was sulfur detected. It is possible that higher interfacial stress developed after a complete α-Al_2O_3 layer established and this high stress caused the oxide to lose coherency with the underlying alloy. Further changes at the interface may be efforts that continue to relax the oxide growth stress.

The amount of sulfur on interfacial voids increased with void size asymptotically from more than 0.5 monolayer to as high as 1.5 monolayers (Fig. 6). Condensation of sulfur-containing vapor species inside the voids at the oxidation temperature onto their surfaces during cooling could not account for the large increase. The observed increase is believed to be a result of void growth,[26] indicating that excess sulfur accumulated at the pore surface as the pores grew. Results in Fig. 7c show that cosegregation of Al and S took place on void faces, causing the sulfur content on the voids to increase, probably forming a 2-dimensional Al-S structure. Steps, as those seen on the upper right corner of the void shown in Fig. 3, were often present on void surfaces. The occurrence of such large surface steps is known to be closely related to high levels of surface sulfur segregation.[36,37] Since growth of these pores is achieved by Al-vapor transport across the pore to the oxide,[26] S cosegregation with Al to the surface followed by Al evaporation can then leave excess S on the surface and, hence, more S on larger pores.

Evaluating the relationships between the surface Fe, Al, and S contents on each area (Fig. 7 and Table II) provides an indication of how S is present at the interface. At the oxide grain-imprinted facets, where the oxide scale was in contact with the alloy prior to the AES observation, the amount of segregated sulfur was no more than 0.5 monolayer. Furthermore, it must

have bonded with Fe, since the Al surface concentration at these locations and at this level of S coverage remained the same as that on the original alloy. This result confirms a previous conclusion drawn from X-ray photoelectron spectroscopy studies[28] that S at the interface was bonded to the Fe in the FeAl alloy, while Al was bonded with O. After the sulfur coverage was greater than ~0.5 monolayer, additional S adsorbed on top of Al, thus quickly decreasing the Al surface concentration, i.e., the Al Auger signal being attenuated by the adsorbed sulfur. On void surfaces, cosegregation of Al and S occurred, so that the observed Al concentration no longer changed with a further S increase. Evaporation of Al from the void surface to supply scale growth above large voids then left excess S on the void surfaces.

CONCLUSIONS

Examinations of the alloy and oxide sides of Al_2O_3–alloy interfaces that formed by oxidizing a Fe–40 at.% Al alloy at 1000°C using Auger-electron spectroscopy showed evidence of sulfur segregation at the interface. While sulfur quickly segregated to interfacial-void surfaces, on areas where the scale was in contact with the alloy prior to the analyses, it was only detected after a complete layer of α-Al_2O_3 established at the interface. The amount then gradually built up with oxidation time to a saturation level of about 4 at.%, or close to half a monolayer. The level of segregation at oxide–alloy interfaces depended strongly on the interface microstructure. As the interface continued to change with oxide growth, it became more accessible to sulfur segregation, indicating a likely relationship between segregation energies and interface microstructure.

The first segregated sulfur at the interface bonded with Fe. A further increase in sulfur, found only on void surfaces, caused more than a monolayer of coverage due to the cosegregation of S and Al, followed by Al evaporation from the void faces to sustain scale growth.

ACKNOWLEDGMENT

Research sponsored by the U.S. Department of Energy under contract No. DE-AC03-76SF00098.

REFERENCES

1. P. A. Douben and A. Miller, eds. in *Surface Segregation Phenomena*, 1st edn (CRC Press, Boca Raton, FL, 1990).
2. R. W. Balluffi R. W., in *Interfacial Segregation*, W. C. Johnson and J. M. Blakely, eds. (ASM, Materials Park, OH, 1977), p. 193.

3. P. Lejcek, A. V. Krajnikov, Yu. N. Ivashchenko, and J. Adamek, *Surf. Sci*, **269/270**, 1147 (1992).
4. J. D. Rittner and D. N. Seidman, *Acta Mater*. **45**, 3191 (1997).
5. D. T. Jayne and J. L. Smialek, *Micros. Oxid*. 2, **183** (1994).
6. W. C. Johnson and J. M. Blakely, *Interfacial Segregation* eds., in (ASM, Materials Park, OH, 1977).
7. K. S. Shin and M. Meshii, *Acta Metall*. **31**, 1559 (1983).
8. C. A. Hippsley, *Acta Metall*. **35**, 2399 (1987).
9. A. W. Funkenbusch, J. G. Smeggil, and N. S. Bornstein, *Metall. Trans*. **16A**, 1164 (1985).
10. J. L. Smialek, *Metall. Trans*. **22A**, 739 (1991).
11. J. L. Smialek, D. T. Jayne, J. C. Schaeffer, and W. H. Murphy, *Thin Solid Films* **253**, 285 (1994).
12. G. H. Meier, F. S. Pettit, and J. L. Smialek, *Werkst. Korros*. **46**, 232 (1995).
13. P. Y. Hou and J. L. Smialek, *Scripta Metall. Mater*. **33**, 1409 (1995).
14. P. Y. Hou and J. L. Smialek, *Mater. High Temp*. **17**, 79 (2000).
15. J. L. Smialek, *Metall. Trans. A* **18A**, 164 (1987).
16. J. G. Smeggil, *Mater. Sci. Eng*. **87**, 261 (1987).
17. H. J. Grabke, D. Wiemer, and H. Viefhaus, *Appl. Surf. Sci*. **47**, 243 (1991).
18. P. Y. Hou, in *High Temperature Corrosion and Materials Chemistry*, P. Y. Hou, M. J. McNallan, R. Oltra, E. J. Opila, and D. A. Shores, eds. (Electrochem. Soc., Pennington, NJ, 1998), p. 198.
19. P. Y. Hou, *J. Mater. Sci. Lett*. **19**, 577 (2000).
20. P. Y. Hou, *Mater. Corros*. **51**, 329 (2000).
21. P. Y. Hou, *Mater. Sci. Forum* **369–372**, 23 (2001).
22. P. Y. Hou and J. Stringer, *Oxid. Met*. **38**, 323 (1992).
23. J. L. Smialek, J. Doychak, and D. J. Gaydosh, *Oxid. Met*. **34**, 259 (1990).
24. J. C. Yang, E. Schumann, I. Levin, and M. Rühle, *Acta Mater*. **46**, 2195 (1998).
25. P. Y. Hou, K. Prüßner, D. H. Fairbrother, J. G. Roberts, and K. B. Alexander, *Scripta Mater*. **40**, 241 (1999).
26. P. Y. Hou, Y. Niu, and C. Van Lienden, *Oxid. Met*., in press.
27. L. E. Davis, N. C. MacDonald, P. W. Palmburg, G. E. Riach, and R. E. Weber, *Handbook of Auger Electron Spectroscopy*, 2nd edn. (Perkin-Elmer Corp., Minnesota MN, 1976).
28. P. Y. Hou and G. D. Ackerman, *Appl. Surf. Sci*. **178**, 156 (2001).
29. D. Briggs and M. P. Seah, eds., in *Practical Surface Analysis*, 2nd edn., Vol. 1, Auger and X-ray Photoelectron Spectroscopy (Wiley, New York, 1990).
30. H. J. Schmutzler, H. Viefhaus, and H. J. Grabke, *Surf. Interanal*. **18**, 581 (1992).
31. W. Gao, C.-H. Xu, and S. Li, *Corros. Sci*. **43**, 671 (2001).
32. B. H. Rabin and R. N. Wright, *Metall. Trans. A* **22A**, 277 (1991).
33. P. Fox, D. G. Lees, and G. W. Lorimer, *Oxid. Met*. **36**, 491 (1991).
34. K. Prüßner, E. Schumann, and M. Rühle, in *Fundamental Aspects of High Temperature Corrosion*, D. A. Shores, R. A. Rapp, and P. Y. Hou, eds. (Electrochem. Soc., Pennington, NJ, 1996), p. 344.
35. J. C. Yang, E. Schumann, H. Mullejans, and M. Rühle, *J. Phys. D Appl. Phys*. **29**, 1716 (1996).
36. J. C. Dunphy, C. Knight, P. Sautet, D. F. Ogletree, G. A. Somorjai, and M. B. Salmeron, *Surf. Sci*. **280**, 313 (1993).
37. J. S. Lin, H. Cabibil, and J. A. Kelber, *Surf. Sci*. **395**, 30 (1998).